www.nature.com/cdd

CDDpress

ARTICLE

Check for updates

H3K36 methyltransferase NSD1 protects against osteoarthritis through regulating chondrocyte differentiation and cartilage homeostasis

Rui Shao[1,5], Jinlong Suo[1,5], Zhong Zhang[2,5], Mingxiang Kong[3], Yiyang Ma[1], Yang Wen[2], Mengxue Liu[1], Lenan Zhuang[4], Kai Ge[4], Qing Bi[3], Changqing Zhang[1]✉ and Weiguo Zou[1,2]✉

Osteoarthritis (OA) is one of the most common joint diseases, there are no effective disease-modifying drugs, and the pathological mechanisms of OA need further investigation. Here, we show that H3K36 methylations were decreased in senescent chondrocytes and age-related osteoarthritic cartilage. *Prrx1-Cre* inducible *H3.3K36M* transgenic mice showed articular cartilage destruction and osteophyte formation. Conditional knockout $Nsd1^{Prrx1\text{-}Cre}$ mice, but not $Nsd2^{Prrx1\text{-}Cre}$ or $Setd2^{Prrx1\text{-}Cre}$ mice, replicated the phenotype of *K36M/+; Prrx1-Cre* mice. Immunostaining results showed decreased anabolic and increased catabolic activities in $Nsd1^{Prrx1\text{-}Cre}$ mice, along with decreased chondrogenic differentiation. Transcriptome and ChIP-seq data revealed that *Osr2* was a key factor affected by *Nsd1*. Intra-articular delivery of *Osr2* adenovirus effectively improved the homeostasis of articular cartilage in $Nsd1^{Prrx1\text{-}Cre}$ mice. In human osteoarthritic cartilages, both mRNA and protein levels of NSD1 and OSR2 were decreased. Our results indicate that NSD1-induced H3K36 methylations and OSR2 expression play important roles in articular cartilage homeostasis and OA. Targeting H3K36 methylation and OSR2 would be a novel strategy for OA treatment.

Cell Death & Differentiation (2024) 31:106–118; https://doi.org/10.1038/s41418-023-01244-8

INTRODUCTION

Osteoarthritis (OA) is a progressive degenerative joint disease that affects nearly half of the elderly population worldwide and represents a major socioeconomic challenge [1, 2]. During the progression of OA, articular cartilage undergoes cellular changes, matrix degradation, structural destruction and even cartilage disappearance [3]. Normal articular cartilage contains a highly specialized cell type, the chondrocytes, which are responsible for extracellular matrix (ECM) production and cartilage homeostasis maintenance by producing enzymes, inflammatory factors and growth factors [4, 5]. Chondrocyte differentiation begins with the recruitment and condensation of Prrx1-positive mesenchymal cells, followed by the proliferation and differentiation of chondroprogenitor cells [6, 7]. When chondrogenic differentiation encounters abnormal conditions, the function and homeostasis of articular cartilage is compromised, which can ultimately lead to OA [8]. Understanding how chondrogenic differentiation and cartilage homeostasis are regulated will provide insights into novel therapeutic strategies for OA.

Methylation of Lys36 on histone H3 (H3K36) has been described to be associated with active chromatin, alternative splicing, dosage compensation, DNA replication, etc. [9, 10]. H3K36 methylation is regulated by methyltransferases and demethylases. H3K36 methyltransferases include NSD1, NSD2, NSD3, SETD2, SMYD2 and so on. The H3K36M mutant induces chondroblastoma formation and sarcoma genesis through dysregulation of chondrogenic differentiation and cartilage formation [11, 12], supporting the role of H3K36 methylation in chondrogenic differentiation. Among the H3K36 methyltransferases, nuclear receptor-binding SET domain-containing protein 1 (NSD1, KMT3B), with its catalytic SET domain [13], is responsible for mono- and di-methylation of H3K36. Heterozygous, truncating mutations/deletions or loss-of-function of NSD1 are associated with two autosomal dominant overgrowth genetic disorders, Sotos syndrome and Beckwith-Wiedemann syndrome [14, 15]. These two disorders display overgrowth of long bones such as arms and legs, but their specific pathogenic mechanisms are unknown [16]. It has been speculated that the overgrowth in patients with Sotos syndrome may be due to the effects of NSD1 mutations on chondrocyte differentiation [17]. Our recent studies have found that NSD1 promotes chondrogenic differentiation at the growth plate to regulate skeletal development and bone fracture repair [18]. Articular cartilage and growth plate chondrocytes have different programs, which also means that the molecular interaction networks in the two cellular taxa will be dramatically different [19]. However, it remains unknown whether H3K36 methylation and NSD1 play a

[1]Institute of Microsurgery on Extremities, and Department of Orthopedic Surgery, Shanghai Sixth People's Hospital Affiliated to Shanghai Jiao Tong University School of Medicine, Shanghai 200233, China. [2]State Key Laboratory of Cell Biology, CAS Center for Excellence in Molecular Cell Sciences, Shanghai Institute of Biochemistry and Cell Biology, Chinese Academy of Sciences; University of Chinese Academy of Sciences, Shanghai 200031, China. [3]Department of Orthopedics, Rehabilitation center, Zhejiang Provincial People's Hospital, Hangzhou, Zhejiang 310014, China. [4]Adipocyte Biology and Gene Regulation Section, National Institute of Diabetes and Digestive and Kidney Diseases, NIH, Bethesda, MD 20892, USA. [5]These authors contributed equally: Rui Shao, Jinlong Suo, Zhong Zhang. ✉email: zhangcq@sjtu.edu.cn; zouwg94@sibcb.ac.cn

Received: 17 August 2023 Revised: 31 October 2023 Accepted: 14 November 2023
Published online: 27 November 2023

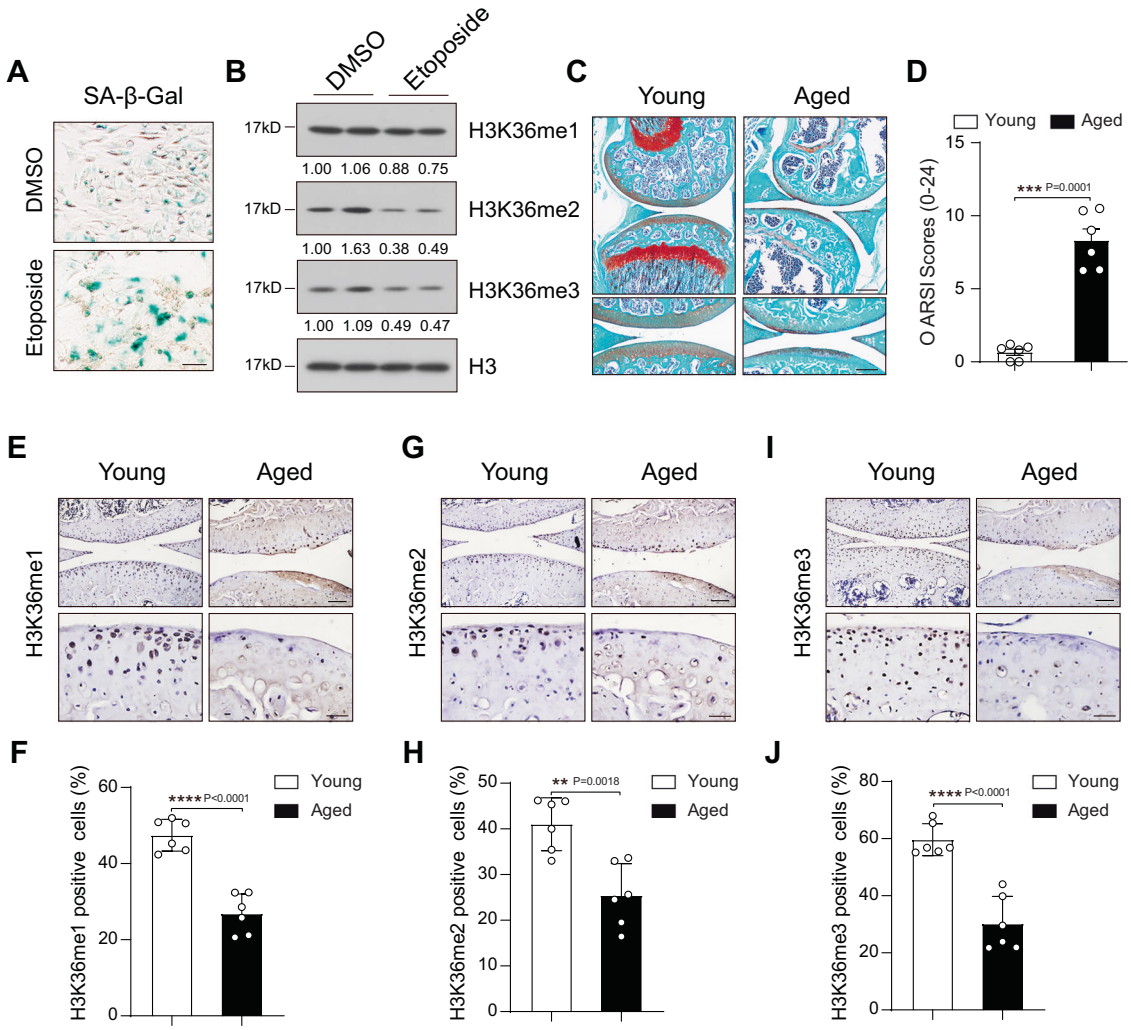

Fig. 1 H3K36 methylations decreased in aged cells and articular cartilage. A SA-β-Gal staining results of ATDC5 cells treated with DMSO or Etoposide. Scale bar = 200 μm. **B** Western blot results of H3K36 methylations in ATDC5 cells treated with DMSO or Etoposide. Safranin O staining results (**C**) and OARSI Scores (**D**) of knee joint sections from two-month-old (Young) and two-year-old (Aged) mice (Young, $n = 6$; Aged, $n = 6$). Scale bar (top) = 200 μm, scale bar (bottom) = 50 μm. Immunohistochemistry results of H3K36me1 (**E**), H3K36me2 (**G**), and H3K36me3 (**I**) and quantification of positive cells ((**F**) for H3K36me1, (**H**) for H3K36me2, (**J**) for H3K36me3) in the articular cartilages from young and aged mice (Young, $n = 6$; Aged, $n = 6$). Scale bar (top) = 200 μm, scale bar (bottom) = 50 μm. Data are expressed as mean ± SD. Unpaired *t* test (**D**, **F**, **H**, **J**).

role in cartilage homeostasis and OA. NSD1's molecular interplay network in articular cartilage remains unknown.

Here, we investigated the functional roles of H3K36 methylation and NSD1 in cartilage homeostasis and OA pathology and firm up a new molecular mechanism different from that in cartilage at the growth version. Our work elucidates that the histone methyltransferase NSD1 regulates chondrogenic differentiation, cartilage homeostasis and the occurrence of OA by regulating Odd-skipped related 2 (OSR2) expression through H3K36 methylation, and establishes the relationship between NSD1 and OSR2 expression in human OA.

RESULTS

H3K36 methylations were decreased in age-induced osteoarthritic articular cartilage

The incidence of OA increases with age, and senescent cells clearance may attenuate OA development [20]. First, we screened for various histone methylation changes in senescent chondrogenic ATDC5 cells induced with Etoposide [21]. SA-β-Gal staining revealed chondrocyte senescence in the etoposide treated group (Fig. 1A). Screening for different histone H3 methylation levels in chondrocyte senescence, H3K36 methylations, including mono-, di-, and tri-methylation, showed different degrees of downregulation, which caught our attention (Fig. 1B and Fig. S1A). In two-year-old mice, osteoarthritic phenotypes such as articular cartilage destruction were observed (Fig. 1C). Accordingly, the OARSI score was higher in aged mice compared to younger mice (Fig. 1D). Immunohistochemistry (IHC) results and statistical data showed that the levels of H3K36me1, H3K36me2 and H3K36me3 were all decreased in the articular cartilage of aged mice (Fig. 1E-J). Taken together, these data suggest that H3K36 methylations were decreased in senescent chondrocytes and age-induced osteoarthritic articular cartilage, and these clues establish a direct association between reduced H3K36 methylation and age-related OA.

Mice with K36M transgenic or *Nsd1* knockout developed OA

H3K36 methylation is regulated by both methyltransferase and demethylase. Prrx1-positive mesenchymal stem cells (MSCs) can differentiate into chondrocytes and give rise to articular cartilage during postnatal development in vivo (Fig. S2A). In order to

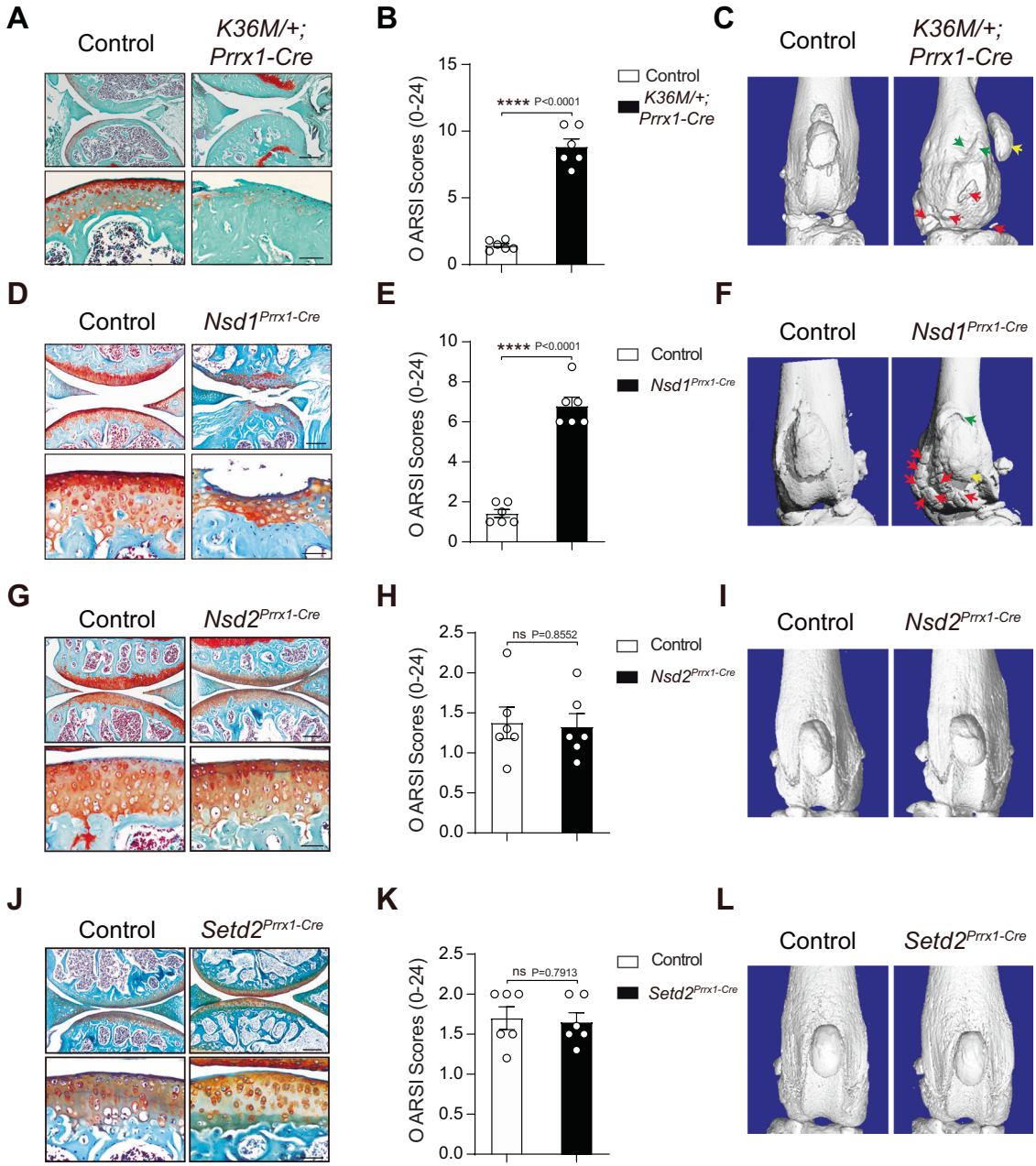

Fig. 2 Mice with *K36M* transgenic or *Nsd1* knockout developed osteoarthritis. Safranin O staining results (**A**, **D**, **G**, **J**), OARSI Scores (**B**, **E**, **H**, **K**), and CT images (**C**, **F**, **I**, **L**) of six-month-old *K36M/+; Prrx1-Cre* mice (**A**–**C**), $Nsd1^{Prrx1\text{-}Cre}$ mice (**D**, **E**), $Nsd2^{Prrx1\text{-}Cre}$ mice (**G**–**I**), $Setd2^{Prrx1\text{-}Cre}$ mice (**J**–**L**), and littermates (control, $n = 6$; *K36M/+; Prrx1-Cre*, $n = 6$; $Nsd1^{Prrx1\text{-}Cre}$, $n = 6$; $Nsd2^{Prrx1\text{-}Cre}$, $n = 6$; $Setd2^{Prrx1\text{-}Cre}$, $n = 6$). Scale bar (top) = 200 μm, scale bar (bottom) = 50 μm. Yellow arrow indicates dislocation of the patella. Green arrows indicate twisted subchondral bone. Red arrows indicate osteophytes. Data are expressed as mean ± SD. Unpaired *t* test (**B**, **E**, **H**, **K**).

explore whether H3K36 methylation is related to OA, we introduced *K36M* transgenic mice [22] and crossed them with *Prrx1-Cre* mice to achieve H3K36 methylation knockdown in MSCs. Consistent with previous reports, three H3K36 methylation levels were decreased in the articular cartilage of *K36M/+; Prrx1-Cre* mice (Fig. S3A). Safranin O and Fast Green (SO) staining results showed the destruction of articular cartilage and lack of proteoglycan in *K36M/+; Prrx1-Cre* mice (Fig. 2A). The OARSI score was also higher than that of wild-type littermates (Fig. 2B). In the knee joint of *K36M/+; Prrx1-Cre* mice, we could see not only osteophyte formation, but also patellar dislocation and subchondral bone distortion (Fig. 2C). These results support that decreased H3K36 methylation in articular chondrocytes leads to OA.

To identify the specific H3K36 methyltransferase that is responsible for articular homeostasis and OA, we constructed $Nsd1^{Prrx1\text{-}Cre}$, $Nsd2^{Prrx1\text{-}Cre}$ and $Setd2^{Prrx1\text{-}Cre}$ mice respectively to detect the articular cartilage development and OA phenotype. From the SO staining results, we could see the articular cartilage destruction in $Nsd1^{Prrx1\text{-}Cre}$ mice (Fig. 2D) and the OARSI score was correspondingly higher (Fig. 2E) but no difference in $Nsd2^{Prrx1\text{-}Cre}$ mice or $Setd2^{Prrx1\text{-}Cre}$ mice (Fig. 2G–L). The knee joint structure was obviously distorted, including dislocated patella, rough and uneven subchondral bone, and abundant osteophyte formation in $Nsd1^{Prrx1\text{-}Cre}$ mice (Fig. 2F and Fig. S4A–F), similar to the phenotypes of *K36M/+; Prrx1-Cre* mice. These results suggest that *Nsd1* knockout mice mimic the OA

phenotype of *K36M/+; Prrx1-Cre* mice, but *Nsd2* or *Setd2* knockout mice do not develop OA.

Nsd1 deficiency disrupted the articular cartilage homeostasis

Articular cartilage homeostasis is maintained by the balance between anabolic and catabolic metabolism and plays a pivotal role in the development of OA [23, 24]. Since NSD1 deficiency in $Prrx1^{+}$ cells resulted in spontaneous OA, we proposed that the articular cartilage homeostasis is disrupted in $Nsd1^{Prrx1\text{-}Cre}$ mice. To investigate the underlying histological changes in articular cartilage of $Nsd1^{Prrx1\text{-}Cre}$ mice, we performed IHC staining to detect metabolic changes in chondrocytes. NSD1 IHC results revealed deletion of NSD1 in the articular chondrocytes of $Nsd1^{Prrx1\text{-}Cre}$ mice (Fig. 3A). In early formed articular cartilage, *Nsd1* knockout resulted in loss of proteoglycan, an important anabolic product, in the superficial and middle layers of articular cartilage (Fig. 3B). With BrdU (5-bromo-2′-deoxyuridine, commonly used for cell proliferation study) injection, the articular cartilage of $Nsd1^{Prrx1\text{-}Cre}$ mice showed more BrdU-positive cells (Fig. 3C, D). TUNEL (terminal deoxynucleotidyl transferase dUTP nick end labeling) staining results showed that there was no difference in cell death between control and $Nsd1^{Prrx1\text{-}Cre}$ mice articular cartilage (Fig. S5A). SOX9, a key regulator of chondrogenic differentiation, was downregulated after *Nsd1* knockout (Fig. 3E, F). The major anabolic metabolite, type II collagen (COL2), was also downregulated (Fig. 3E, F). Levels of enzymes involved in the articular cartilage catabolism were increased, including MMP3, MMP13 and ADAMTS5 (Fig. 3E, F). We also performed immunostaining in the other three mouse models to detect metabolic changes in articular cartilages. The results showed no significant changes in the staining results of *Nsd2* and *Setd2* mouse models, except for the staining results of *K36M/+; Prrx1-Cre* mice, which were consistent with those of $Nsd1^{Prrx1\text{-}Cre}$ mice (Fig. S6A–C). This is consistent with the OA phenotype we observed. The senescence marker P16 staining results showed a significant increase of senescent cells in the knee joint sections of two mouse models, $Nsd1^{Prrx1\text{-}Cre}$ and *K36M/+; Prrx1-Cre*, while the changes were not significant in the other two animal models (Fig. S7A). This is consistent with our findings that methylation of H3K36 changes significantly during chondrocyte senescence, but the enzymes actually involved in chondrocyte homeostasis are mainly NSD1 rather than NSD2 and SETD2. Collectively, these data indicate that NSD1 is an important regulator of chondrogenic differentiation and cartilage metabolic balance.

Disturbed cell proliferation, differentiation and metabolism after NSD1 knockout

To elucidate the underlying mechanisms of impaired chondrocyte cellular and metabolic changes in $Nsd1^{Prrx1\text{-}Cre}$ mice, we performed RNA-seq in $Nsd1^{fl/fl}$ primary chondroprogenitor cells infected with Egfp and Cre lentiviruses. There were 544 differentially expressed genes (DEGs), of which 366 were downregulated and 178 were upregulated (Fig. 4A, B). Gene Ontology (GO) enrichment analysis of these DEGs indicated that cell differentiation, negative regulation of cell proliferation, extracellular matrix organization, and cartilage development were the top enriched biological process (BP) terms for downregulated genes in Cre cells (Fig. 4C). To assess the signaling pathways enriched in these DEGs, we performed KEGG pathway analysis. We identified metabolic pathways as the most enriched KEGG pathway in downregulated genes in Cre cells (Fig. 4D). In order to understand the changes of gene sets in Egfp and Cre cells, we performed gene set enrichment analysis (GSEA). Notably, Cre cells were preferentially enriched for cell proliferation-related processes, including G1-to-S phase transition signaling and Hippo signaling (Fig. 4E), whereas Egfp cells were enriched for extracellular matrix assembly and reactive oxygen species biosynthetic processes (Fig. 4F). During the cell cycle, G1 phase transition to S phase is crucial for the control of eukaryotic cell proliferation [25]. Hippo signaling was a key regulator of cell proliferation, fate decision, tissue growth and regeneration [26]. Functionally, DEGs involved in metabolic pathways included glutathione metabolism, protein glycosylation, response to hypoxia, lipid metabolism and glycolytic process, most of which were validated by RT-PCR (Fig. 4G and Fig. S8). Overall, our data suggest that NSD1 knockout reprograms the transcriptome of chondroprogenitor cells, resulting in increased proliferation, decreased differentiation, and decreased anabolism, leaving articular cartilage in an immature state.

Osr2 was regulated by *Nsd1* through H3K36 methylation

NSD1 is an H3K36 methyltransferase and H3K36 methylation modifications usually positively regulate gene transcription [9]. Next, we performed ChIP-seq using an antibody specific for H3K36me2 with $Nsd1^{fl/fl}$ chondroprogenitor cells infected with Egfp or Cre virus (Fig. 5A). Through cross-analysis of RNA-seq and ChIP-seq results, there were 139 genes that showed downregulated expression and decreased H3K36me2 enrichment in Cre cells compared to Egfp cells (Fig. 5B). Among the overlapping genes, there were 4 transcription factors: *Osr2*, *Sox5*, *Mitf*, *Sox9* and *Osr2* showed the most significant decrease (Fig. 5C). *Osr2*, a zinc finger-containing transcription factor, plays a role in regulating *Sox9* and promoting fin chondrogenesis [27]. *Osr2* is expressed in the cells of the developing synovial joint and $Osr2^{-/-}$ mice showed fused tarsal elements [28]. In this study, OSR2 was downregulated in the articular cartilage of $Nsd1^{Prrx1\text{-}Cre}$ mice (Fig. 5D-E). To further verify the necessity of *Osr2* for chondrocyte homeostasis, we used shRNA to knock down *Osr2* in primary chondroprogenitor cells, followed by chondrogenic differentiation. As shown by Alcian blue staining, chondroprogenitor cells showed decreased chondrogenic differentiation after *Osr2* knockdown (Fig. 5F, G). Marker genes related to chondrogenic differentiation and anabolism were decreased (Fig. 5H), and cartilage catabolism related enzymes were increased after *Osr2* knockdown (Fig. 5I). We next investigated the relationship between NSD1-mediated H3K36 methylation and *Osr2* expression. Based on the H3K36me2 binding analysis on the *Osr2* gene (Fig. 5J), we designed primers for ChIP-qPCR analysis of H3K36me1 and H3K36me2 in $Nsd1^{fl/fl}$ primary chondroprogenitor cells infected with Egfp or Cre lentivirus. Both H3K36me1 and H3K36me2 levels on *Osr2* were decreased after *Nsd1* knockout as detected by ChIP-qPCR (Fig. 5K). These data suggest that *Osr2* is regulated by NSD1 through H3K36 methylation to promote chondrogenic differentiation and anabolic metabolism and to inhibit catabolic metabolism.

Enhanced expression of *Osr2* improved chondrogenic differentiation and cartilage homeostasis caused by *Nsd1* deficiency

In order to verify whether *Osr2* regulates chondrogenic differentiation and cartilage homeostasis downstream of NSD1 in vivo, we constructed lentivirus and adenovirus expressing Egfp and *Osr2*. Using primary chondroprogenitor cells obtained from wildtype and $Nsd1^{Prrx1\text{-}Cre}$ mice, we infected *Nsd1* knockout chondro-progenitor cells with Egfp and *Osr2* lentivirus and performed micromass culture to monitor chondrogenic differentiation. Alcian blue staining revealed that overexpression of *Osr2* rescued the NSD1-deficiency-induced defects in chondrogenic differentiation (Fig. 6A). Consistent with these data, the decreased expression of chondrogenic differentiation markers in $Nsd1^{Prrx1\text{-}Cre}$ mice was also rescued by forced *Osr2* overexpression (Fig. 6B, C). Intra-articular injection is often used to test the effects of compounds on articular cartilage. Here, adenovirus expressing Egfp or *Osr2* was injected intra-articularly (Fig. 6D and Fig. S9A) and articular cartilage was harvested. SO staining results showed that the articular cartilage homeostasis was rescued with *Osr2* overexpression, the level of proteoglycan was also restored in $Nsd1^{Prrx1\text{-}Cre}$ mice (Fig. 6E). Anabolism product like COL2 was

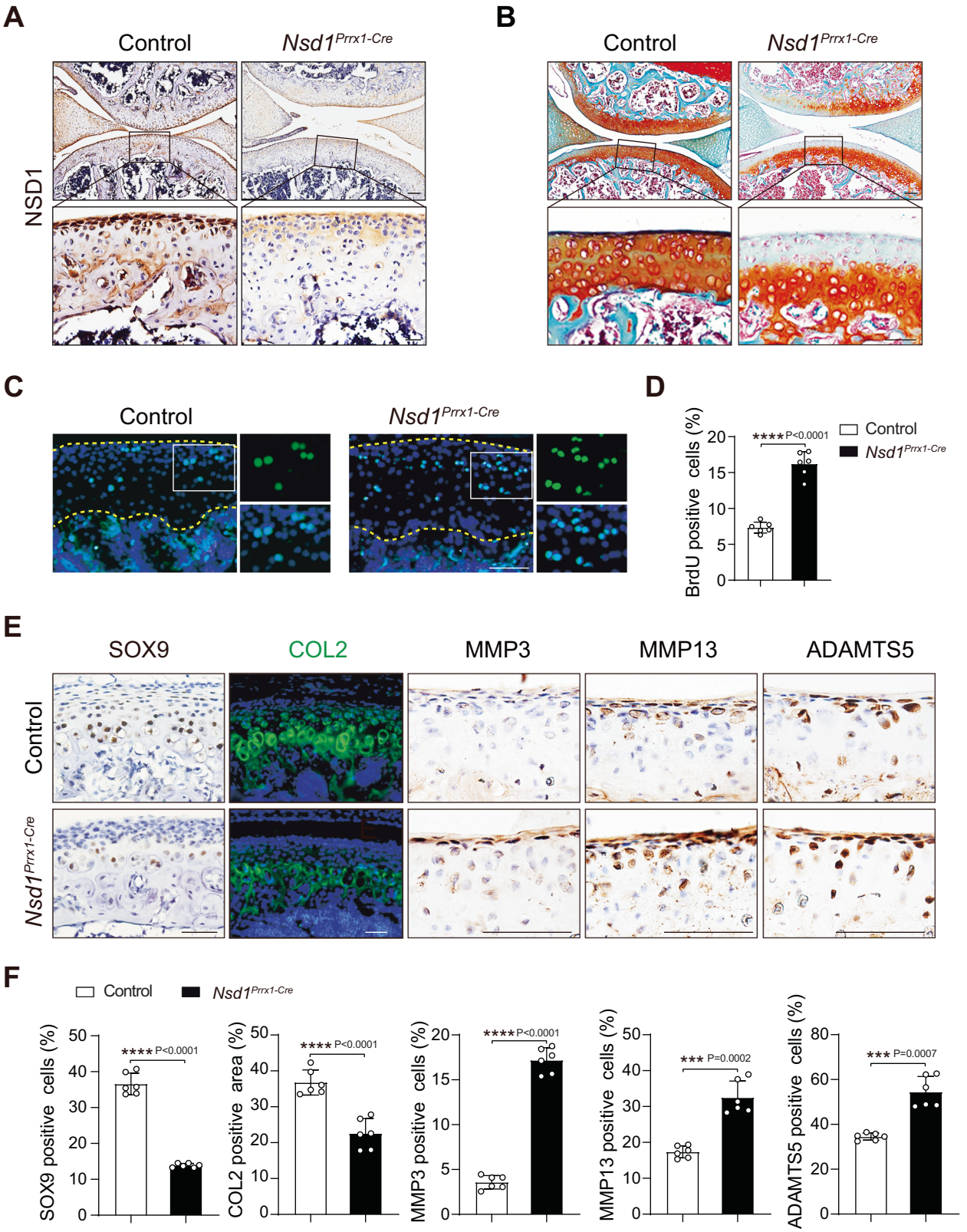

Fig. 3 ***Nsd1*** **deficiency disrupted articular cartilage homeostasis. A** NSD1 IHC results in the articular cartilage sections from one-month-old mice. Scale bar (top) = 100 μm, scale bar (bottom) = 50 μm. **B** Safranin O staining results of knee joint sections from one-month-old *Nsd1*$^{Prrx1\text{-}Cre}$ mice and littermates. Scale bar (top) = 100 μm, scale bar (bottom) = 50 μm. BrdU staining (**C**) and quantification (**D**) results of knee joint sections from one-month-old *Nsd1*$^{Prrx1\text{-}Cre}$ mice and littermates. Scale bar (top) = 100 μm, scale bar (bottom) = 50 μm. **E** Immunostaining results of SOX9 (first column), COL2 (second column), MMP3 (third column), MMP13 (fourth column), ADAMTS5 (fifth column) on knee joint sections from one-month-old mice. Scale bar = 50 μm. **F** Quantification of cells or areas positively stained for SOX9, COL2, MMP3, MMP13, and ADAMTS5 (control, $n = 6$; *Nsd1*$^{Prrx1\text{-}Cre}$, $n = 6$). Data are expressed as mean ± SD. Unpaired *t* test (**D**, **F**).

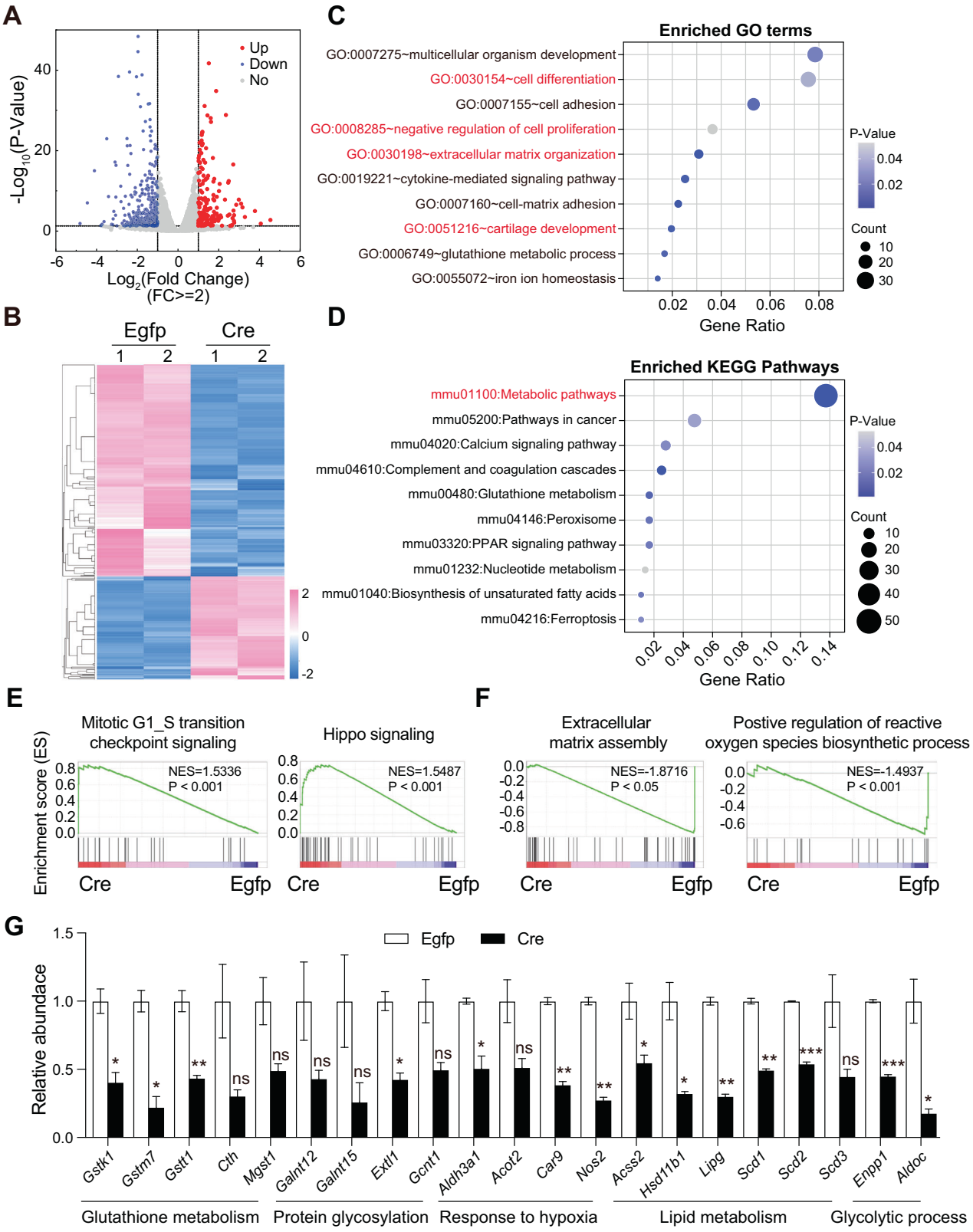

Fig. 4 Disturbed cell proliferation, differentiation and metabolism after NSD1 knockout. Volcano plot (**A**) and heatmap (**B**) showing transcriptome changes of immortalized *Nsd1*$^{fl/fl}$ cells infected with Egfp or Cre virus. Fold change >= 2. Enriched GO terms (**C**) and KEGG pathways (**D**) analysis of downregulated genes in Cre cells. GSEA plots (**E**, **F**) showing enrichment of GO BP between Egfp and Cre cells. **G** RT-PCR analysis of candidate genes expression levels in RNA-seq samples. Data represent the mean ± SD ($n = 4$). *$P < 0.05$, **$P < 0.01$, ***$P < 0.001$, unpaired t test was performed.

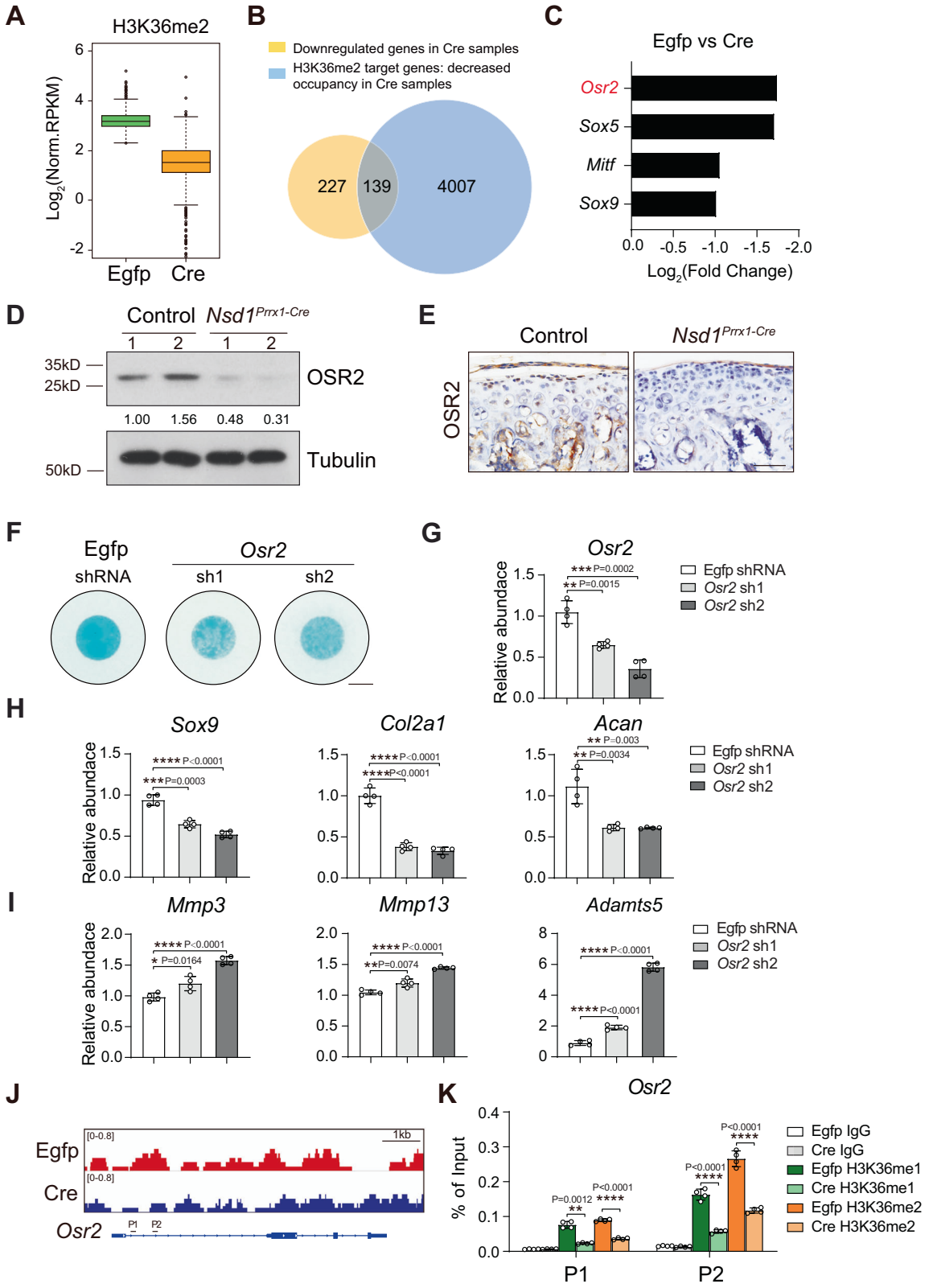

restored to normal level according to the immunostaining results (Fig. 6F). In a word, these results suggest that NSD1 regulation of chondrocyte homeostasis and OA is dependent on *Osr2*, and *Osr2* can rescue *Nsd1* deficiency-induced chondrocyte differentiation disorder and OA.

NSD1 and OSR2 were downregulated in osteoarthritic articular cartilage

To explore whether NSD1 and OSR2 expression is altered in osteoarthritic cartilage, we collected normal and osteoarthritic articular cartilage from samples of OA patients who underwent

Fig. 5 *Osr2* was regulated by NSD1 through H3K36 methylation. A Boxplot showing the binding levels of decreased H3K36me2 binding peaks in Cre samples based on H3K36me2 ChIP-seq with Egfp and Cre cells. **B** Venn diagram showing the overlap of genes with decreased expression and decreased H3K36me2 occupancy in Cre cells. **C** Quantitative expression analysis of four transcription factors in the RNA-seq samples. Western blot (**D**) and IHC (**E**) results of OSR2 in articular cartilage of one-month-old $Nsd1^{Prrx1\text{-}Cre}$ mice and littermates. Scale bar = 50 μm. **F** Alcian blue staining of wildtype chondroprogenitor cells infected with Egfp shRNA or *Osr2* shRNA. Scale bar = 2 mm. **G** qRT-PCR results showing the knockdown efficiency of *Osr2* ($n = 4$ for each treatment). qRT-PCR results showing the levels of genes related to chondrogenic differentiation and anabolic metabolism (**H**) and catabolic metabolism (**I**) in cells infected with Egfp shRNA or *Osr2* shRNA ($n = 4$ for each treatment). **J** H3K36me2 binding peaks from the H3K36me2 ChIP-seq of immortalized $Nsd1^{fl/fl}$ cells infected with Egfp or Cre virus. **K** ChIP-qPCR analysis of H3K36me1 and H3K36me2 bindings in immortalized $Nsd1^{fl/fl}$ cells infected with Egfp or Cre virus ($n = 4$ for each assay). Data are expressed as mean ± SD. One-way ANOVA (**G**, **H**–**I**, **K**).

knee joint replacement. SO staining revealed destruction of articular cartilage in human samples (Fig. 7A). IHC staining showed that both NSD1 and OSR2 were decreased in osteoarthritic cartilage (Fig. 7B, C). Detection of mRNA levels showed that both *NSD1* and *OSR2* were downregulated in osteoarthritic articular cartilage (Fig. 7D, E). Correlation analysis revealed a strong correlation between *NSD1* and *OSR2* expression (Fig. 7F). Altogether, these findings establish a link between decreased expression of NSD1, OSR2 and OA.

DISCUSSION

Onset and progression of OA are closely related to age and chondrocyte senescence [20, 29]. In this study, we first screened for different histone H3 methylation modifications in senescent chondrocytes and found that all three modifications of H3K36 methylation were all downregulated (Fig. 1B). In the osteoarthritic articular cartilage of aged mice, we also detected decreased levels of all three modifications of H3K36 methylation (Fig. 1E–J). When lysine 36 of histone H3 was mutated to methionine (H3K36M), H3K36 methylations were downregulated, impairing the differentiation of mesenchymal progenitors and causing chondrocytes to exhibit characteristics of cancer cells, including increased proliferation and decreased differentiation, resulting in undifferentiated sarcoma and chondroblastoma [11]. *Prrx1*, a paired-related homeobox transcription factor, also known as *Prx1*, *Pmx*, *MHox*, and *k2*, is expressed in the mesenchyme during embryonic development [30, 31]. Prrx1-positive MSCs can differentiate into chondrocytes and give rise to articular cartilage in vivo [32]. The chondrocytes in the articular cartilage were all derived from Prrx1-positive cells (Fig. S2A). We obtained *K36M/+; Prrx1-Cre* mice to study the effects of H3K36 methylation knockdown on chondrocytes and articular cartilage homeostasis. OA phenotype observed in *K36M/+; Prrx1-Cre* mice confirmed the relationship between H3K36 methylation and OA.

Different H3K36 methyltransferases are responsible for different methylation modifications, and these enzymes also have their own protein functions [9]. Most H3K36 methyltransferases are responsible for the mono- and di-methylation of H3K36, NSD1 mutations have been reported to affect bone growth in Sotos syndrome patients [16], and conditional knockout of *Nsd1* in MSCs resulted in delayed skeletal development and fracture repair [18]. NSD2 mutations and loss of function also resulted in developmental delay [33, 34]. SETD2 has long been the only enzyme responsible for catalyzing the tri-methylation of H3K36 [35], and recently SMYD5 was found to also able to catalyze the trimethylation of H3K36 in the promoter region of the gene [36]. SETD2 has been reported to regulate the fate of bone marrow MSCs [37]. To further clarify which H3K36 methylation modification and its corresponding enzyme(s) are associated with OA, we selected genes that have been reported to be associated with skeletal development or the endochondral ossification process from the enzymes responsible for catalyzing H3K36 mono- & dimethylation or trimethylation to further construct mice. We examined the articular cartilage phenotype in $Nsd1^{Prrx1\text{-}Cre}$, $Nsd2^{Prrx1\text{-}Cre}$ and $Setd2^{Prrx1\text{-}Cre}$ mice respectively and found that only *Nsd1* knockout was able to reproduce the phenotype of *K36M/+; Prrx1-Cre* mice (Fig. 2). Our previous study found that $Nsd1^{Prrx1\text{-}Cre}$ mice showed delayed early skeletal development with abnormal formation of the primary ossification center and secondary ossification center [18]. $Nsd1^{Prrx1\text{-}Cre}$ mice also displayed delayed bone fracture healing with impaired callus formation [18]. *Nsd1* knockout cartilage progenitor cells showed increased proliferation and decreased differentiation capacity with decreased expression of *Sox9*, a key transcription factor for chondrogenic differentiation [18]. The current study demonstrated that NSD1 deficiency in articular cartilage could lead to an OA phenotype with attenuated articular cartilage anabolism and enhanced articular cartilage catabolism (Figs. 2, 3).

In NSD1 knockout primary chondroprogenitor cells, *Osr2* expression and genomic occupancy of H3K36me1 and H3K36me2 were decreased (Figs. 4, 5). *Osr2*, a zinc finger-containing transcription factor, belongs to the odd-skipped family and plays a role in the regulating *Sox9* and promoting fin chondrogenesis [27]. Mice lacking *Osr2* exhibited supernumerary tooth development in the molars by regulating the expression of BMP4 [38]. *Osr2* is expressed in developing articular synovial cells, and $Osr2^{-/-}$ mice showed fused tarsal elements [28]. In our study, *Osr2* was regulated by *Nsd1* through H3K36me1 and H3K36me2 binding on the genomic region, and *Osr2* knockdown resulted in decreased chondrogenic differentiation, decreased anabolism, and increased catabolism (Fig. 5). Overexpression of *Osr2* not only restored the decreased chondrocyte differentiation, but also rescued the cartilage homeostasis after *Nsd1* knockout, especially with more COL2 distribution in the superficial zone of articular cartilage (Fig. 6). Thus far, the role of *Osr2* in chondrogenic differentiation and OA has been fully elucidated in cellular and animal models. Interestingly, we also found decreased levels of NSD1 and OSR2 in human osteoarthritic articular cartilage (Fig. 7). These suggest that NSD1 and OSR2 may be potential mediators linking risk factors to OA development.

During the analysis of RNA-seq data, there were 48 metabolism-related genes (Fig. S8A), which were further subjected to Gene Ontology analysis, including Biological Pathway (BP), Cellular Component (CC), and Molecular Function (MF) analysis, and the results are detailed in Fig. S8B, C. Bioinformatics analysis revealed that these metabolism-related genes were mainly involved in the metabolic processed of lipid, glutathione, protein glycosylation, and response to hypoxia, all of which are associated with cartilage development, homeostasis maintenance, or OA development. Lipids are nutrients for chondrocytes and are involved in cartilage growth, injury, and regeneration in diverse ways [39]. There is high lipid biosynthesis during chondrogenesis and specific fatty acid could decrease proteinase involved in cartilage matrix degradation [40]. Glutathione is an important regulator of cellular redox potential and oxidative damage, and functions as a mediator between oxidative stress resistance and resilience in the cartilage during the aging process and OA [41]. Protein glycosylation is associated with chondrocyte senescence in the pathogenesis of OA [42]. Cartilage is a chronically hypoxic tissue and cellular responses to hypoxia are not only related to cell survival, but also affect specific functions of chondrocytes. Hypoxia can modulate the main cartilage matrix genes, including *Col2a1*, *Acan*, and *Col9* through regulating SOX9 [43].

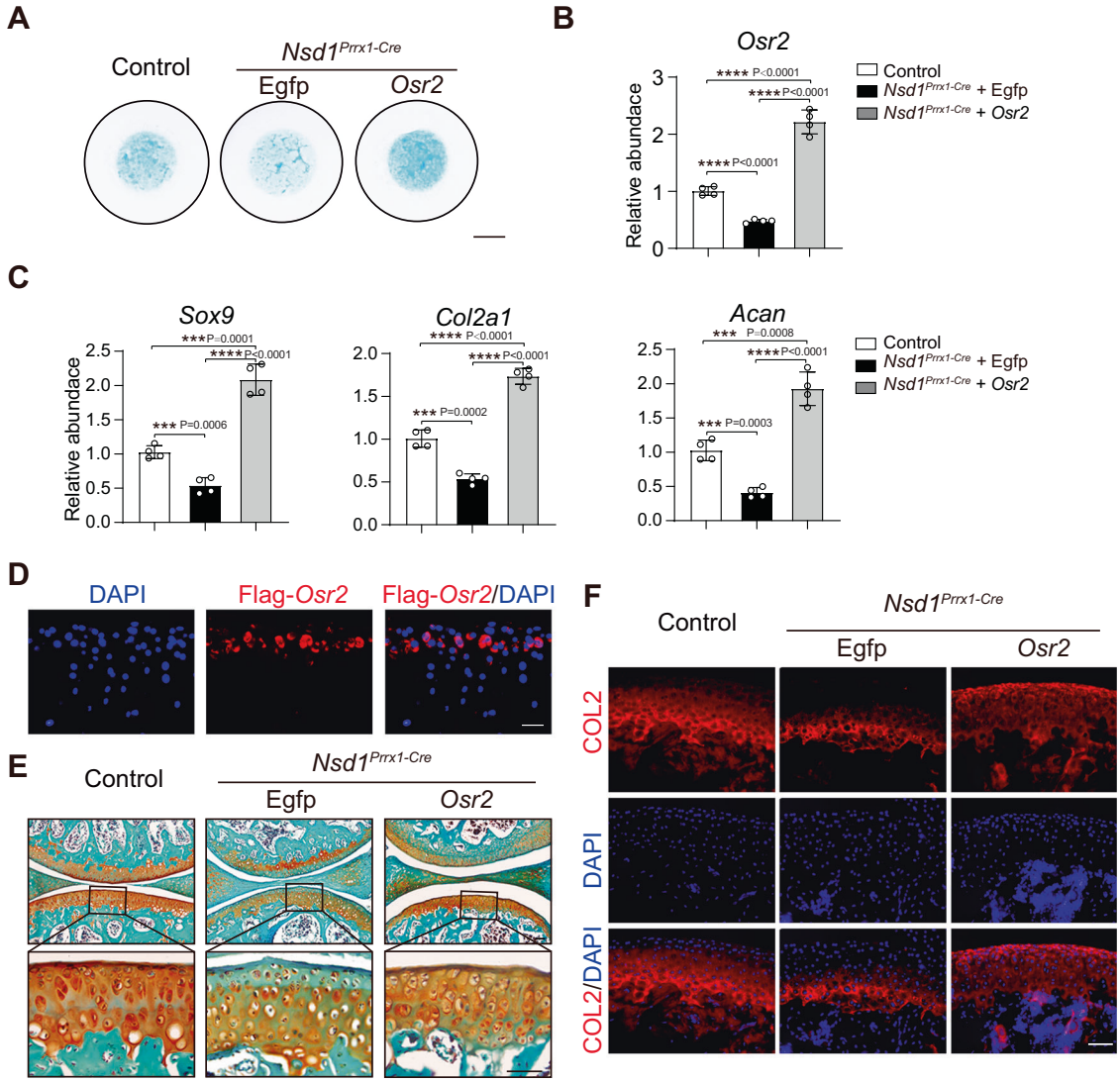

Fig. 6 *Osr2* complement could rescue the defect in chondrogenic differentiation and cartilage homeostasis caused by *Nsd1* knockout. **A** Alcian blue staining results of micromass with chondroprogenitor cells from control and $Nsd1^{Prrx1\text{-}Cre}$ mice, infected with Egfp or *Osr2* lentivirus. Scale bar = 2 mm. **B** qRT-PCR results showing the overexpression efficiency of *Osr2* (control, $n = 4$; $Nsd1^{Prrx1\text{-}Cre}$ + Egfp, $n = 4$; $Nsd1^{Prrx1\text{-}Cre}$ + *Osr2*, $n = 4$). **C** qRT-PCR results showing the levels of genes related to chondrogenic differentiation and anabolic metabolism (control, $n = 4$; $Nsd1^{Prrx1\text{-}Cre}$ + Egfp, $n = 4$; $Nsd1^{Prrx1\text{-}Cre}$ + *Osr2*, $n = 4$). **D** Distribution of OSR2-positive cells in the articular cartilage of mice with intra-articular injection of Flag-*Osr2* adenovirus. Scale bar = 50 μm. **E** Safranin O staining results of knee joint sections from wildtype and $Nsd1^{Prrx1\text{-}Cre}$ mice intra-articularly injected with Egfp or *Osr2* adenovirus. Scale bar (top) = 100 μm, scale bar (bottom) = 50 μm. **F** COL2 IF results of knee joint sections from control and $Nsd1^{Prrx1\text{-}Cre}$ mice intra-articularly injected with Egfp or *Osr2* adenovirus. Scale bar = 50 μm. Data are expressed as mean ± SD. One-way ANOVA (**B**, **C**).

In summary, we elucidate for the first time the role of H3K36 methylation and NSD1 in OA from a genetic perspective. We revealed a novel epigenetic molecular regulatory pathway in articular cartilage and established a direct link between the NSD1-*Osr2* axis and osteoarthritis (Fig. 7G). Currently, osteoarthritis drugs focus on pain relief and inflammation reduction, with few drugs available that can effectively inhibit the osteoarthritic process and repair damaged joint tissue [44, 45]. Intra-articular drug delivery has several advantages over systemic administration, and a number of promising treatments are in clinical development, including small molecules, gene therapies, biologic therapies, and devices [46]. Securing NSD1/H3K36me3/*Osr2* levels in combination with intra-articular injections may be a promising treatment for OA, and more research data is needed before this can be done. This work provides a potential epigenetic therapeutic strategy for the treatment of OA.

MATERIALS AND METHODS

Mice

The $Nsd1^{fl/fl}$ mice [18], *Prrx1-Cre* mice [18, 37] and $Setd2^{fl/fl}$ mice [37] were mentioned before. *K36M/+* mice were provided by Dr. Kai Ge (National Institutes of Health). $Nsd2^{fl/fl}$ mice were provided by Dr. Jun Qin (Shanghai Institute of Nutrition and Health, CAS). All mice analyzed were maintained on the C57BL/6 background and monitored in a specific pathogen–free (SPF) environment. Experiments were carried out under the approval of the Institutional Animal Care and Use Committee (IACUC) of the CAS Center for Excellence in Molecular Cell Sciences, Chinese Academy of Sciences.

Cell culture

Primary chondroprogenitor cells were obtained from the femoral condyles and tibial plateau of newborn mice. Cartilages were digested with 1 mg/ml collagenase II (Sigma, C6885) for two hours at 37 °C and the digestions were discarded. The left tissues were digested with half concentration of collagenase II overnight at 37 °C and the digestions were filtered with 70 μm cell strainer (Falcon, 352350) the next day. The cells were plated into

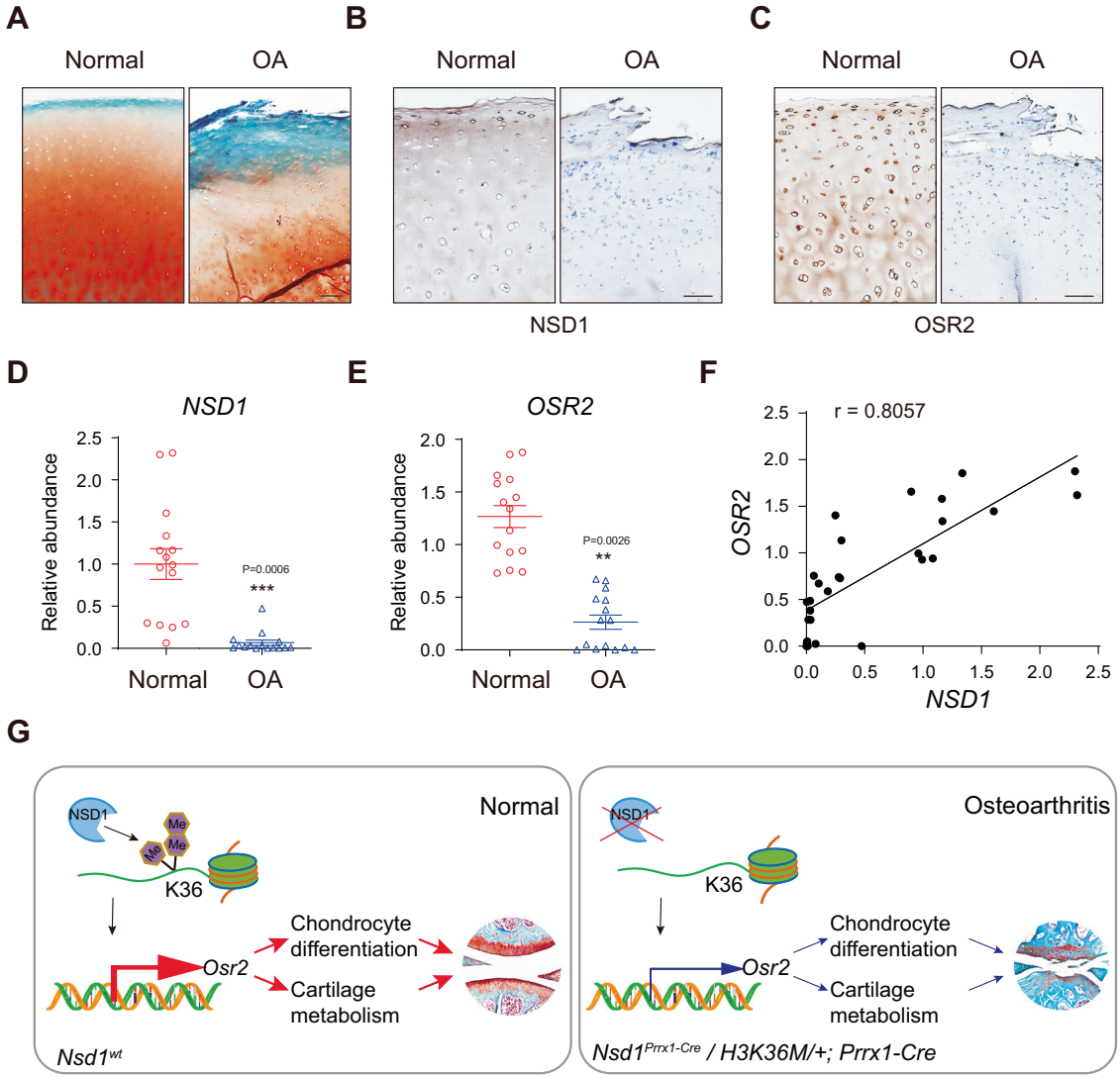

Fig. 7 NSD1 and OSR2 were decreased in osteoarthritic cartilage. A Safranin O staining results of normal and osteoarthritic cartilage from knee joint replacement samples. Scale bar = 100 μm. Immunohistochemistry results of NSD1 (**B**) and OSR2 (**C**) in normal and osteoarthritic cartilage from knee joint replacement samples. Scale bar = 100 μm. qRT-PCR results of NSD1 (**D**) and OSR2 (**E**) in normal and osteoarthritic cartilage from knee joint replacement samples (Normal, $n = 15$; OA, $n = 15$). **F** Correlation analysis between the expression level of NSD1 and OSR2 in all samples. The coefficient value was labeled. **G** Schematic model of NSD1-H3K36me1/2-*Osr2* in the regulation of chondrocyte differentiation and cartilage metabolism. Data are expressed as mean ± SEM. Unpaired *t* test (**D**, **E**).

α-MEM medium (Corning, 10-022-CVR) supplemented with 10% fetal bovine serum (FBS) and 1% penicillin/streptomycin.

Micromass culture

Micromass culture was performed when primary chondrocytes reached 80–90%. Digested and suspended chondrocytes to 1×10^7cells/ml, plated a droplet of 12.5 μl cell suspension to the central of 12-well-plate, let the plate stand at 37 °C for two hours and then gently added the chondrogenic differentiation medium, which contains DMEM, 10 ng/ml TGFβ3 (Peprotech, 100-36E), 100 nM dexamethasone (Sigma, D1756), 50 μg/ml L-ascorbic acid 2-phosphate (Sigma, A8960), 1 mM sodium pyruvate (Sigma, 25-000-CIR), 40 μg/ml proline (Sigma, P5607) and 1% ITS (Cyagen, ITSS-10201-10). Micromass at different time was acidified with 0.1 N HCl and then stained with 1% alcian blue (Sigma, A5268).

Senescent chondrocyte model

Chondrogenic cell line (ATDC5) was treated with the DNA-damaging agent etoposide ("DNA damage-induced senescence", DIS). We confirmed the induction of the senescence phenotype in these cells by evaluation senescence-associated β-galactosidase (SA-β-Gal) staining.

Histology and immunohistochemistry

Knee joints from mice were fixed in 4% paraformaldehyde for 48 h, decalcified in 10% EDTA and embedded in paraffin and cut into 8μm thick sections. Immunohistochemistry was performed using Vector Rabbit kit according to the manufacturer's instructions. Images were captured using a microscope (Olympus BX51, Tokyo, Japan).

Immunofluorescence

Sections were blocked in PBS with 10% horse serum for 1 h and then stained overnight with specific antibody. Secondary antibodies were used according to the species of primary antibody. DAPI (sigma, D8417) was used for counterstaining. Slides were mounted with anti-fluorescence mounting medium (Dako, S3023) and images were acquired with Olympus BX51 microscope or Leica SP8 confocal microscope.

BrdU assay

Three-week-old mice were injected with BrdU (Sigma, B5002) at 50 mg/kg, repeated the injection every two days, three times in total and collected the knee samples on the 7th day after first injection. Fixed, decalcified and embedded the samples in paraffin, cut into 5 μm thick sections. Sections

were first soaked in formamide/SSC (1:1) buffer for 1 hour at 65 °C to repair the antigen. Then soaked in 2 N HCl for 30 min at 37 °C to open the DNA double strands after rinsed with PBS. Rinsed and soaked the sections in 0.01 M Tris-HCl for 10 min to reconstruct the alkaline environment. Then blocked with 5% sheep serum for 2 h at room temperature. Incubated sections with BrdU antibody (Cell Signaling, Bu20a) overnight at 4 °C. The next day rinsed the sections and incubated with secondary antibody for 2 h at room temperature. Rinsed and stained the nucleus with Hoechst 33342 for 10 min. Rinsed and mounted the sections. Images were obtained by Olympus BX51.

TUNEL assay

TUNEL apoptosis assay was performed on paraffin sections following the instructions of the DeadEnd™ Fluorometric TUNEL System (Promega, G3250), using PI (Thermo, P1304MP) staining as a positive control.

Human articular cartilage samples

Human articular cartilage samples were obtained with the informed consent of the patients and the approval of the ethics committee of Shanghai Sixth People's Hospital and Zhejiang Provincial People's Hospital. Samples were obtained from individuals undergoing total knee arthroplasty and subjected to RNA extraction and paraffin embedding and sectioning.

μCT analysis

Mouse knee joints were collected, soft tissues removed and fixed in 70% ethanol. Samples were scanned with a Scanco μCT80 (SCANCO Medical, Swiss) or Skyscan 1272 scanner (Bruker, Germany) at a resolution of 10 μm. Bone erosion and osteophyte analysis were performed according to the protocol provided by PerkinElmer, Inc (Application Note: MicroCT Investigation of Bone Erosin and Deformation in an Osteoarthritic Rat Model).

Antibodies

H3K36M (Arigo, ARG57228), NSD1 (Bioss, bs-8170R), COL2 (Abcam, ab34712), H3K36me1 (Abcam, ab9048), H3K36me2 (Abcam, ab9049), H3K36me3 (Abcam, ab9050), SOX9 (Millipore, AB5535), OSR2 (sc-393516), MMP3 (Abcam, ab52915), MMP13 (Abcam, ab39012), ADAMTS5 (Thermo Fisher, PA5-27165), H3K4me1 (Abcam, ab176877), H3K4me2 (Abcam, ab7766), H3K4me3 (Abcam, ab213224), H3K9me1 (Abcam, ab176880), H3K9me3 (Active Motif, 61013), H3K27me1 (Abcam, ab194688), H3K27me2 (Abcam, ab24684), H3K27me3 (Abcam, ab6002), H3K79me1 (Abcam, ab2886), H3K79me2 (Abcam, ab3594).

Western blot

Tissues or cells were harvested and lysed with EBC buffer (1% NP-40, 10% glycerol, 135 nM NaCl, 20 mM Tris pH8.0) containing protease inhibitors. Then lysates were separated through running SDS-PAGE gel and blotting on PVDF membrane (Bio-Rad). After incubation with specific antibodies, we used enhanced chemiluminescence kit (Millipore) to detect the protein signals. Our method of quantification is to do a ratio between the destination bands and their matching internal reference bands after quantification. The ratio of each destination band is then normalized and presented below each destination band.

Real-time PCR analysis

Total RNA was isolated from different tissues and cells with TRIzol Reagent (Sigma, T9424) and reverse-transcribed with the PrimeScript RT Reagent Kit (Takara, RR037A). The real-time reverse transcriptase (RT)-PCR reaction was performed with the Bio-Rad CFX Connect Real-Time System. The primer sets used were mouse *Gstk1*: sense 5′-GGTCCTATGCAGATACCAACAC-3′ and anti-sense 5′-GTACTGGCCTTTTCGGGGAA-3′; mouse *Gstm7*: sense 5′-ATGAT GCGGCTTTACTCCGAG-3′ and anti-sense 5′-GCCCCAAATAGC-CATCTTTGTG- 3′; mouse *Gstt1*: sense 5′-CCGTCGCGCCATTTATATCTT-3′ and anti-sense 5′-CCCTCTTCATGGGGTTCACC-3′; mouse *Cth*: sense 5′-TTCCTGCCTAGTT TCCAGCAT-3′ and anti-sense 5′-GGAAGTCCTGCT-TAAATGTGGTG-3′; mouse *Mgst1*: sense 5′-CTCAGGCAGCTCATGGACAAT-3′ and anti-sense 5′-GTTAT CCTCTGGAATGCGGTC-3′; mouse *Galnt12*: sense 5′-TCAACATCTATCTGAGC GACCG-3′ and anti-sense 5′-CTTGGGCAGGTTATCA-TAATCGT-3′; mouse *Galnt15*: sense 5′-GCTCCACAACACTGGATTTGG-3′ and anti-sense 5′-GTGTG CTCCAGGTTCTGTTG-3′; mouse *Extl1*: sense 5′-TTCTGGCTGGCGTTGTCAG -3′ and anti-sense 5′-GGGTTCGTCTCAGACTG GGA-3′; mouse *Gcnt1*: sense 5′-ACTTGTTTCGGAGGAGACTTTTC-3′ and anti-sense 5′-GGGTCACCCTGTAA AATCTTGGT-3′; mouse *Aldh3a1*: sense 5′-AATATCAGTAGCATCGTGAACCG-3′ and anti-sense 5′-GGAGAGCCCCT-TAATCGTGAAA-3′; mouse *Acot2*: sense 5′-GTTGTGCCAACAGGATTGGAA-3′ and anti-sense 5′-GCTCAGCGTCGCATTT GTC-3′; mouse *Car9*: sense 5′-TGCTCCAAGTGTCTGCTCAG-3′ and anti-sense 5′-CAGGTGCATCCTCTT-CACTGG-3′; mouse *Nos2*: sense 5′-GTTCTCAGCCC AACAATACAAGA-3′ and anti-sense 5′-GTGGACGGGTCGATGTCAC-3′; mouse *Acss2*: sense 5′-AAACACGCTCAGGGAAAATCA-3′ and anti-sense 5′-ACCGTA GATG-TATCCCCCAGG-3′; mouse *Hsd11b1*: sense 5′-CAGAAATGCTCCAG GGAAA-GAA-3′ and anti-sense 5′-GCAGTCAATACCACATGGGC-3′; mouse *Lipg*: sense 5′-ATGCGAAACACGGTTTTCCTG-3′ and anti-sense 5′-GTAGCTGGTAC TCCAGTGGG-3′; mouse *Scd1*: sense 5′-TTCTTGCGATACACTCTGGTGC-3′ and anti-sense 5′-CGGGATTGAATGTTCTTGTCGT-3′; mouse *Scd2*: sense 5′-GCATTTGGGAGCCTTGTACG-3′ and anti-sense 5′-AGCCGTGCCTTGTATG TTCTG-3′; mouse *Scd3*: sense 5′-GTTGCCACTTTACTGAGATACGC-3′ and anti-sense 5′-GAAGCCCTCGCCCATACTT-3′; mouse *Enpp1*: sense 5′-CTGGT TTTGTCAGTATGTGTGCT-3′ and anti-sense 5′-CTCACCGCACCTGAATTTGTT -3′; mouse *Aldoc*: sense 5′-AGAAGGAGTTGTCGGATATTGCT-3′ and anti-sense 5′-TTCTCCACCCCAATTTGGCTC-3′; mouse *Col2*: sense 5′-CGGTCCTACGG TGTCAGG-3′ and anti-sense 5′-GCAGAGGA CATTCC CAGTGT-3′; mouse *Sox9*: sense 5′-TTCCTCCTCCCGGCATGAGTG-3′ and anti-sense 5′-CAACTTTGCC AGCTTGCACG-3′; mouse *Acan*: sense 5′-AATCCCCAAATCCCTCATAC-3′ and anti-sense 5′-CTTAGTCCA CCCCTCCTCAC-3′; mouse *Osr2*: sense 5′-CTCAC CAATTACTCCTTCCTGC-3′ and anti-sense 5′-GCACCGCACTGAGACCATAG-3′; mouse *Mmp3*: sense 5′-ACATGGAGACTTTGTCCCTTTTG-3′ and anti-sense 5′-TTGGCTGAGTGGTA-GAGTCCC-3′; mouse *Mmp13*: sense 5′-CTTCTTCTTG TTGAGCTGGACTC-3′ and anti-sense 5′-CTGTGGAGGTCACTGTAGACT-3′; mouse *Adamts5*: sense 5′-GGAGCGA GGCCATTTACAAC-3′ and anti-sense 5′-CGTAGACAAGGTAGCC CACTTT-3′; human *NSD1*: sense 5′-AGCAAAGAAA TGAAGTGGACGG-3′ and anti-sense 5′-TGAATGTGTGTTAATCAACGGA-3′, human *OSR2*: sense 5′-TCCGCCTAAGATGGGAGACC-3′ and anti-sense 5′-GGTAAAGTGTCTGCC GCAAAA-3′.

ChIP-Seq and ChIP-qPCR

Nsd1$^{fl/fl}$ primary chondrocytes were infected with lentivirus expressing Egfp and Cre respectively. After puromycin treatment, Egfp and Cre expressing primary chondrocytes were fixed with 1% formaldehyde for 10 min and terminated with glycine for 5 min (final concentration = 0.125 M). After twice washing with precooled PBS (protease inhibitor containing), cells were scraped and resuspended in SDS-lysis buffer respectively (50 mM Tris-HCl Ph 7.5, 10 mM EDTA, 1% SDS and protease inhibitor) and sonicated. Cells were centrifuged to obtain cell extracts, which were then added to pre-cleaned protein G agarose and rotated for at 4 °C 1 h. Extracts were centrifuged and supernatants were collected into new tubes. ChIP assay was performed using H3K36me1/2 antibody. Normal IgG was used as negative control. The raw sequencing data is store on the Figshare site (https://doi.org/10.6084/m9.figshare.22774088). ChIP-qPCR was used to amplify different regions of the target gene genome using the following primers: *Osr2* P1: sense 5′-AGTCCCGGGCCTCGTGTTCT-3′ and anti-sense 5′-TCTTGCCGAATGCGTAAATCT-3′. *Osr2* P2: sense 5′-TGAAATGGAGAGGGA GGGAGCGGA-3′ and anti-sense 5′-ACGA AGTTTCTGCCCCTTCCCCGT-3′.

Lentiviruses and infection

Lentiviruses expressing Egfp and mouse *Osr2* were constructed by inserting the gene CDS into the Plenti vector. Virus package was prepared according to the VSVG - delta 8.9 system. Mouse primary chondrocytes were cultured for two days, infected with lentivirus for forty-eight hours, digested, and passed to micromass culture.

Adenoviruses and intra-articular injection

The CDS of Egfp and mouse *Osr2* were cloned into pYr-1.1. Then the LR recombination reactions were performed between the plasmid (pYr-1.1-Egfp/*Osr2*) and the destination vector (pAd/BL-DEST) using LR Clonase II (Invitrogen, 12538120). Finally, HEK293A cells were transfected with PacI linearized adenovirus vectors (pAd-Egfp/*Osr2*) to generate recombinant adenoviruses Ad-Egfp/*Osr2*. Cerium chloride gradient centrifugation was used to harvest purified and concentrated adenoviruses. Intra-articular (IA) injection of Ad-*Osr2* (2×10^8 plaque-forming units in a total volume of 5 μl) was performed once a week for 6 weeks in 4-week-old male mice; IA injection of Ad-Egfp was used as a control. Mice were sacrificed 4 days after the last IA injection for histologic analysis.

Statistical analysis

Quantitative data were presented as the mean ± SD or mean ± SEM and analyzed by unpaired *t* test (two-tailed) or one-way ANOVA using GraphPad Prism 6 software. $P < 0.05$ was considered as statistically significant. Specific *P* values for each significance of difference test were indicated in the graphs. Correlation assay was conducted with GraphPad.

DATA AVAILABILITY

All data generated or analyzed during this study are included in this published article (and its Supplementary information files). The datasets used and/or analyzed during the current study are available from the corresponding author on reasonable request.

REFERENCES

1. Hunter DJ, March L, Chew M. Osteoarthritis in 2020 and beyond: a Lancet Commission. Lancet. 2020;396:1711–2.
2. Sharma L. Osteoarthritis of the Knee. N Engl J Med. 2021;384:51–9.
3. Mahmoudian A, Lohmander LS, Mobasheri A, Englund M, Luyten FP. Early-stage symptomatic osteoarthritis of the knee - time for action. Nat Rev Rheumatol. 2021;17:621–32.
4. Simkin PA. A biography of the chondrocyte. Ann Rheum Dis. 2008;67:1064–8.
5. Carballo CB, Nakagawa Y, Sekiya I, Rodeo SA. Basic science of articular cartilage. Clin Sports Med. 2017;36:413–25.
6. Pittenger MF, Mackay AM, Beck SC, Jaiswal RK, Douglas R, Mosca JD, et al. Multilineage potential of adult human mesenchymal stem cells. Science. 1999;284:143–7.
7. Barry F, Boynton RE, Liu B, Murphy JM. Chondrogenic differentiation of mesenchymal stem cells from bone marrow: differentiation-dependent gene expression of matrix components. Exp Cell Res. 2001;268:189–200.
8. Chen D, Shen J, Zhao W, Wang T, Han L, Hamilton JL, et al. Osteoarthritis: toward a comprehensive understanding of pathological mechanism. Bone Res. 2017;5:16044.
9. Wagner EJ, Carpenter PB. Understanding the language of Lys36 methylation at histone H3. Nat Rev Mol Cell Biol. 2012;13:115–26.
10. Xu L, Zhao Z, Dong A, Soubigou-Taconnat L, Renou JP, Steinmetz A, et al. Di- and Tri- but not monomethylation on histone H3 lysine 36 marks active transcription of genes involved in flowering time regulation and other processes in arabidopsis thaliana. Mol Cell Biol. 2023;28:1348–60.
11. Fang D, Gan H, Lee JH, Han J, Wang Z, Riester SM, et al. The histone H3.3K36M mutation reprograms the epigenome ofchondroblastomas. Science. 2016;352:1344–8.
12. Lu C, Jain SU, Hoelper D, Bechet D, Molden RC, Ran L, et al. Histone H3K36 mutations promote sarcomagenesis through altered histone methylation landscape. Science. 2016;352:844–9.
13. Rayasam GV, Wendling O, Angrand PO, Mark M, Niederreither K, Song L, et al. NSD1 is essential for early post-implantation development and has a catalytically. EMBO J. 2003;22:3153–63.
14. Kurotaki N, Imaizumi K, Harada N, Masuno M, Kondoh T, Nagai T, et al. Haploinsufficiency of NSD1 causes Sotos syndrome. Nat Genet. 2002;30:365–6.
15. Baujat G, Rio M, Rossignol S, Sanlaville D, Lyonnet S, Le Merrer M, et al. Paradoxical NSD1 Mutations in Beckwith-Wiedemann Syndrome and 11p15 Anomalies in Sotos Syndrome. Am J Hum Genet. 2004;74:715–20.
16. Agwu JC, Shaw NJ, Kirk J, Chapman S, Ravine D, Cole TRP. Growth in Sotos syndrome. Arch Dis Child. 1999;80:339–42.
17. Visser R, Landman EB, Goeman J, Wit JM, Karperien M. Sotos syndrome is associated with deregulation of the MAPK/ERK-signaling pathway. PLoS One. 2012;7:e49229.
18. Shao R, Zhang Z, Xu Z, Ouyang H, Wang L, Ouyang H, et al. H3K36 methyltransferase NSD1 regulates chondrocyte differentiation for skeletal development and fracture repair. Bone Res. 2021;9:30.
19. Haseeb A, Kc R, Angelozzi M, de Charleroy C, Rux D, Tower RJ, et al. SOX9 keeps growth plates and articular cartilage healthy by inhibiting chondrocyte dedifferentiation/osteoblastic redifferentiation. Proc Natl Acad Sci USA. 2021;118:e2019152118.
20. Jeon OH, Kim C, Laberge RM, Demaria M, Rathod S, Vasserot AP, et al. Local clearance of senescent cells attenuates the development of post-traumatic osteoarthritis and creates a pro-regenerative environment. Nat Med. 2017;23:775–81.
21. Fafian-Labora JA, Rodriguez-Navarro JA, O'Loghlen A. Small extracellular vesicles have GST activity and ameliorate senescence-related tissue damage. Cell Metab. 2020;32:71–86.e5.
22. Zhuang L, Jang Y, Park YK, Lee JE, Jain S, Froimchuk E, et al. Depletion of Nsd2-mediated histone H3K36 methylation impairs adipose tissue development and function. Nat Commun. 2018;9:1796.
23. Lian WS, Wu RW, Ko JY, Chen YS, Wang SY, Yu CP, et al. Histone H3K27 demethylase UTX compromises articular chondrocyte anabolism and aggravates osteoarthritic degeneration. Cell Death Dis. 2022;13:538.
24. Wang C, Shen J, Ying J, Xiao D, O'Keefe RJ. FoxO1 is a crucial mediator of TGF-beta/TAK1 signaling and protects against osteoarthritis by maintaining articular cartilage homeostasis. Proc Natl Acad Sci USA. 2020;117:30488–97.
25. Bertoli C, Skotheim JM, de Bruin RA. Control of cell cycle transcription during G1 and S phases. Nat Rev Mol Cell Biol. 2013;14:518–28.
26. Ma S, Meng Z, Chen R, Guan KL. The Hippo pathway: biology and pathophysiology. Annu Rev Biochem. 2019;88:577–604.
27. Lam PY, Kamei CN, Mangos S, Mudumana S, Liu Y, Drummond IA. odd-skipped related 2 is required for fin chondrogenesis in zebrafish. Dev Dyn. 2013;242:1284–92.
28. Gao Y, Lan Y, Liu H, Jiang R. The zinc finger transcription factors Osr1 and Osr2 control synovial joint formation. Dev Biol. 2011;352:83–91.
29. Chen X, Gong W, Shao X, Shi T, Zhang L, Dong J, et al. METTL3-mediated m(6)A modification of ATG7 regulates autophagy-GATA4 axis to promote cellular senescence and osteoarthritis progression. Ann Rheum Dis. 2022;81:87–99.
30. Logan M, Martin JF, Nagy A, Lobe C, Olson EN, Tabin CJ. Expression of Cre Recombinase in the developing mouse limb bud driven by a Prxl enhancer. Genesis. 2002;33:77–80.
31. Nohno T, Koyama E, Myokai F, Taniguchi S, Ohuchi H, Saito T, et al. Development biology-A chicken homeobox gene related to drosophila paired is predominantly expressed in the developing limb. Dev Biol. 1993;158:254–64.
32. Bragdon BC, Bennie A, Molinelli A, Liu Y, Gerstenfeld LC. Post natal expression of Prx1 labels appendicular restricted progenitor cell populations of multiple tissues. J Cell Physiol. 2022;237:2550–60.
33. Zanoni P, Steindl K, Sengupta D, Joset P, Bahr A, Sticht H, et al. Loss-of-function and missense variants in NSD2 cause decreased methylation activity and are associated with a distinct developmental phenotype. Genet Med. 2021;23:1474–83.
34. Boczek NJ, Lahner CA, Nguyen TM, Ferber MJ, Hasadsri L, Thorland EC, et al. Developmental delay and failure to thrive associated with a loss-of-function variant in WHSC1 (NSD2). Am J Med Genet Part A. 2018;176:2798–802.
35. Edmunds JW, Mahadevan LC, Clayton AL. Dynamic histone H3 methylation during gene induction: HYPB/Setd2 mediates all H3K36 trimethylation. EMBO J. 2007;27:406–20.
36. Zhang Y, Fang Y, Tang Y, Han S, Jia J, Wan X, et al. SMYD5 catalyzes histone H3 lysine 36 trimethylation at promoters. Nat Commun. 2022;13:3190.
37. Wang L, Niu N, Li L, Shao R, Ouyang H, Zou W. H3K36 trimethylation mediated by SETD2 regulates the fate of bone marrow mesenchymal stem cells. PLoS Biol. 2018;16:e2006522.
38. Zhang Z, Lan Y, Chai Y, Jiang R. Antagonistic actions of Msx1 and Osr2 pattern mammalian teeth into a single row. Science. 2009;323:1232–4.
39. Su Z, Zong Z, Deng J, Huang J, Liu G, Wei B, et al. Lipid metabolism in cartilage development, degeneration, and regeneration. Nutrients. 2022;14:3984.
40. Villalvilla A, Gómez R, Largo R, Herrero-Beaumont G. Lipid transport and metabolism in healthy and osteoarthritic cartilage. Int J Mol Sci. 2013;14:20793–808.
41. Zhu S, Makosa D, Miller B, Griffin TM. Glutathione as a mediator of cartilage oxidative stress resistance and resilience during aging and osteoarthritis. Connect Tissue Res. 2019;61:34–47.
42. Yoshimoto M, Sadamori K, Tokumura K, Tanaka Y, Fukasawa K, Hinoi E. Bioinformatic analysis reveals potential relationship between chondrocyte senescence and protein glycosylation in osteoarthritis pathogenesis. Front Endocrinol. 2023;14:1153689.
43. Murphy CL, Thoms BL, Vaghjiani RJ, Lafont JE. HIF-mediated articular chondrocyte function: prospects for cartilage repair. Arthritis Res Ther. 2009;11:213.
44. Arden NK, Perry TA, Bannuru RR, Bruyere O, Cooper C, Haugen IK, et al. Non-surgical management of knee osteoarthritis: comparison of ESCEO and OARSI 2019 guidelines. Nat Rev Rheumatol. 2021;17:59–66.
45. Sabha M, Hochberg MC. Non-surgical management of hip and knee osteoarthritis; comparison of ACR/AF and OARSI 2019 and VA/DoD 2020 guidelines. Osteoarthritis and Cartilage Open. 4 (2022).
46. Jones IA, Togashi R, Wilson ML, Heckmann N, Vangsness CT. Intra-articular treatment options for knee osteoarthritis. Nat Rev Rheumatol. 2018;15:77–90.

ACKNOWLEDGEMENTS

We thank Dr. Xinyuan Liu (Institute of Biochemistry and Cell Biology, Chinese Academy of Sciences, Shanghai) for providing vectors and reagents related to the adenovirus package. We also thank the members of the Zou lab for helpful discussions.

AUTHOR CONTRIBUTIONS

WZ and RS designed the research; RS, JS, ZZ performed the research; LZ, KG, CZ and QB contributed reagents and analytical tools; MK and QB collected human cartilage samples; RS, JS, ZZ and WZ analyzed the data; RS and WZ wrote the paper.

FUNDING

This work was supported by the National Key Research and Development Program of China (2022YFA1106800, 2022YFA0806600), the National Natural Science Foundation of China (NSFC) (82230082, 81991512, 82202742, 81902212), the Strategic Priority Research Program of the Chinese Academy of Science (XDB0570000), the CAS Project for Young Scientists in Basic Research (YSBR-077), the Shanghai Frontiers Science Center of Degeneration and Regeneration in Skeletal System (BJ1- 9000- 22- 4002).

COMPETING INTERESTS

The authors declare no competing interests.

ETHICS APPROVAL AND CONSENT TO PARTICIPATE

The experimental protocol for animal studies was reviewed and approved by the Institutional Animal Care and Use Committee (IACUC) of the CAS Center for Excellence in Molecular Cell Sciences, Chinese Academy of Sciences. Human articular cartilage samples were obtained with the informed consent of the patients and the approval of the ethics committee of Shanghai Sixth People's Hospital and Zhejiang Provincial People's Hospital.

ADDITIONAL INFORMATION

Supplementary information The online version contains supplementary material available at https://doi.org/10.1038/s41418-023-01244-8.

Correspondence and requests for materials should be addressed to Changqing Zhang or Weiguo Zou.

Reprints and permission information is available at http://www.nature.com/reprints

Publisher's note Springer Nature remains neutral with regard to jurisdictional claims in published maps and institutional affiliations.